DETERMINATION OF THE LINEAR APERTURE OF THE SSC CLUSTERED LATTICE USED FOR THE CONCEPTUAL DESIGN REPORT*

G.F. Dell
Brookhaven National Laboratory, Upton, New York 11973

Summary

A study is made of the linear aperture for the clustered lattice used for the SSC Conceptual Design Report. Random multipole errors are included in all magnetic elements including the insertion dipoles and quadrupoles. Based on the concept of smear, the linear aperture is equal to the dynamic aperture in the range $-0.1 \leq \Delta P/P \leq 0.03\%$. Strong coupling for $\Delta P/P > 0\%$ produces large smears. A variation of the smear parameter that is insensitive to coupling is proposed. A comparison is made with results reported in the SSC Conceptual Design Report.

Introduction

Previous studies have centered upon determining the dynamic aperture of the SSC.[1] This aperture is defined as the maximum initial amplitude for which betatron motion is stable for a specified number of turns--usually 400. There is never any certainty that the dynamic aperture determined for a relative small number of turns represents a condition for which particle motion is stable for indefinitely long periods of time. From an operational point of view, the dynamic aperture is interpreted as that aperture for which motion is stable for a time sufficiently long that measurements and correction schemes can be implemented. For 400 turns the real time is $\sim$ 100 msec.

In addition to the concept of a dynamic aperture that establishes a criterion for short term stability, a second aperture, the linear aperture, has been defined and hopefully indicates the amplitude for which betatron motion is stable indefinitely. Two definitions of linear aperture have been suggested. The first is based on the rms deviation of the Courant-Snyder "invariant" from its initial (or average) value and typically specifies that this deviation be no more than 10%. The second defines the linear aperture to be the betatron amplitude for which the betatron tune deviates from the initial tune (zero amplitude tune) by 0.005. The concept of linear aperture is still exploratory; the limits of 10% and 0.005 are arbitrary and are subject to change.

In the present paper both definitions are used to determine the linear aperture of SSC clustered lattice having two insertions with $\beta^* = 0.5$m and two insertions with $\beta^* = 10$m. This is the lattice described in the SSC Conceptual Design Report (CDR).[2]

The region of tune space selected for SSC operation lies along the principal diagonal and is bounded by $78.250 \leq \nu_z \leq 78.287$ for z = x and y. In the present study a working point of $\nu_x = 78.266$, $\nu_y = 78.283$ has been selected; this is near one of the standard points (78.265, 78.285) used for studies included in the SSC Conceptual Design Report. The study has been made for only one machine (one set of random multipole errors) and is intended to explore the dependence of the linear aperture on momentum. Randon multipole errors are present in all elements, quadrupoles and dipoles, in the insertions as well as the arcs. The random multipoles are those listed in the CDR.[3] For all elements $\sigma b_1 = \sigma a_1 = 0$ and $(\sigma a_n, \sigma b_n) \neq 0$ for $2 \leq n \leq 5$ for quadrupoles and $(\sigma a_n, \sigma b_n) \neq 0$ for $2 \leq n \leq 10$ for dipoles. For the quadrupole triplets near the interaction regions, 90% correction of all multipole errors has been assumed. The magnets used to deflect the beam vertically at the interaction region are of FNAL type and have multipoles that are scaled according to the coil radius.

The magnetic field is represented by:

$$B = B_0 + \Delta B = B_0(1 + \sum_n c_n r^n)$$

where: $c_n = b_n + ia_n$ with b_n and a_n being the normal and skew multipoles,
$r = x = iy$, and
n = multipole order. ($n = 1$ denotes quadrupole)

The random multipole coefficients, σa_n and σb_n, vary as $1/r_0^{n+m}$ with $m = \frac{1}{2}$ for dipoles and $m = -\frac{1}{2}$ for quadrupoles, and r_0 denotes the effective coil radius of the magnet. The kick r' given to a particle is $r' = \Delta B \cdot \ell / B_0 \rho$ with ℓ, B_0, and ρ being the element length, central bending field, and radius of curvature, respectively. Hence for $|r| < r_0$, the kick r' given to the test particle is expected to decrease as the multipole order increases. During tracking a test of the particle's amplitude is made at each sextupole, at the center of each quadrupole, and at both ends of every dipole. For the dynamic aperture, there is no limit to the amplitude of motion--for purposes or tracking, "no limit" is considered to be 1000 mm.

Linear Aperture Determination

In the following discussion a comparison is made between tracking results obtained at $\Delta P/P = \pm 0.1\%$ for a test particle launched at a defocusing arc quadrupole with a radial amplitude of 3.15 mm. The machine tune (ν_x, ν_y) is (78.260,78.281), and the particle tune is (78.261,78.275) at $\Delta P/P = +0.1\%$, and the corresponding tunes at -0.1% are (78.267,78.290) and (78.272,78.292); ν_y at -0.1% is outside the upper bound of y = 78.287. Two sets of four figures are presented for comparison. Figures 1 and 3 contain phase plots at $\Delta P/P = .1\%$ in the horizontal and vertical planes, respectively, and Figures 2 and 4 contain the corresponding phase plots at $\Delta P/P = -.1\%$. Normalized coordinates u and v are used with $u = z/\sqrt{\beta_z}$ and $v = \sqrt{\beta_z}\, z'$ with z = x or y. The resulting phase plots should be circular when no perturbations are present. However, the plots are annular and have a finite thickness which in this case results principally from coupling of motion in the horizontal and vertical planes.

In Figures 5 and 6, the information from the horizontal and vertical phase plots is combined; the abscissa corresponds to $\sqrt{\varepsilon_x}$, and the ordinate corresponds to $\sqrt{\varepsilon_y}$ with ε denoting the emittance. These plots are called smear plots and are used to indicate the relation between the horizontal and vertical emittances on a turn-by-turn basis. The smear plot for $\Delta P/P = .1\%$ shows a much more pronounced variation of the emittances than does the plot for $\Delta P/P = -.1\%$. Finally, in Figures 7 and 8 the dependence of the horizontal and vertical emittances on time (number of turns) is plotted at $\Delta P/P = .1\%$ and $-.1\%$, respectively. The emittance transfer back and forth between the horizontal and vertical planes (coupling) is clearly evident in Figure 7. Figures 1 through 8 are used to develop the arguments of the rest of the paper.

In studies of dynamic aperture, the initial amplitude of the test particle is increased until motion becomes unstable; this is a well defined situation. However, in determining the linear aperture, small variations of tune or emittance are measured, and there is no well defined test that indicates when the linear

*Work performed under the auspices of the U.S. Department of Energy.

This syntax was checked against the command language of the existing programs. It permits to express everything that these programs need to be told. A standard command language can be decoded by a standard decoder which therefore need not be written for each program. Commands can be defined and/or modified from data in the form of command dictionaries. It was found desirable to include enough attributes in the element definitions to cover the needs of several programs. This goes beyond the list of element attributes in the standard element definition language. The attributes should appear in the dictionaries even when they are ignored by some programs. A specific example was the aperture of a quadrupole which is used in the fringe field calculation of MARYLIE.

Uniform Data Structures. Uniform data structures for storing and accessing the description of the machine and the definition of the commands allow the integration of several program modules into an

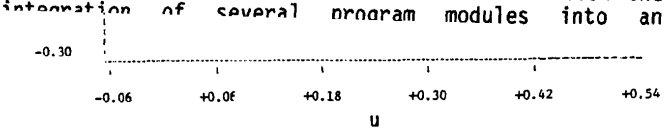

Fig. 1 Phase plot of horizontal motion at $\Delta P/P=+0.1\%$. 1000 turns. $\varepsilon_{x_o}=\varepsilon_{y_o}=0.0225\pi$ mm mradians. Random multipoles in all quadrupoles $(\sigma a_n,\sigma b_n)\neq 0$, $2 \leq n \leq 5$, and dipoles $(\sigma a_n,\sigma b_n)\neq 0$, $2 \leq n \leq 10$. Coupling reduces ε_x to nearly zero.

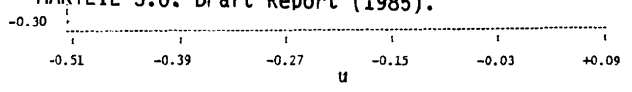

Fig. 2 Phase plot of horizontal motion at $\Delta P/P=-0.1\%$. 1000 turns. $\varepsilon_{x_o}=\varepsilon_{y_o}=0.0225\pi$ mm mradians. Random multipoles in all quadrupoles $(\sigma a_n,\sigma b_n)\neq 0$, $2 \leq n \leq 5$, and dipoles $(\sigma a_n,\sigma b_n)\neq 0$, $2 \leq n \leq 10$. Coupling is indicated by radial width of plot and is much less than that at $\Delta P/P = 0.1\%$.

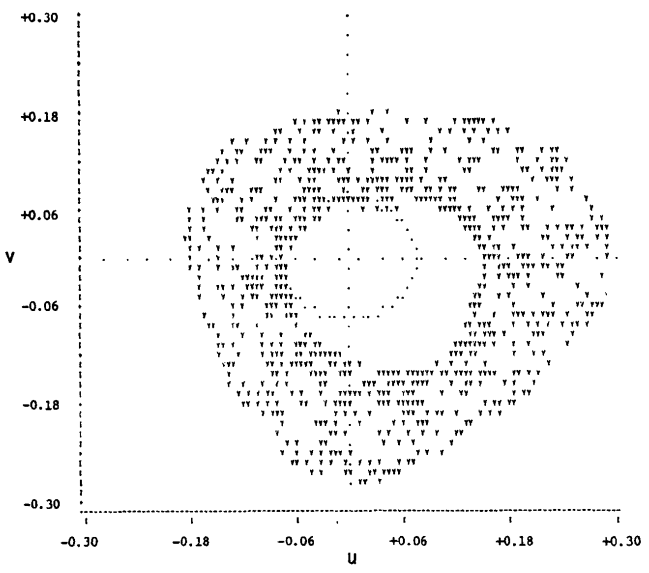

Fig. 3 Phase plot of vertical motion at $\Delta P/P=0.1\%$. (Companion to Fig. 1). Width of plot indicates coupling, but ε_y does not approach zero. Circle (dots) indicates a reference emittance, and lines (dotted) indicate reference axes. Center of plot is displaced indicating nonzero vertical dispersion.

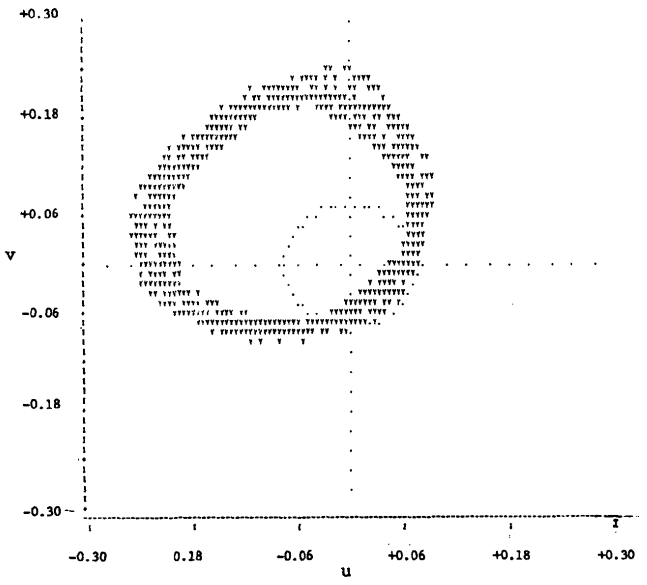

Fig. 4 Phase plot for vertical plane at $\Delta P/P=-0.1\%$. (Companion to Fig. 2). Little coupling is evident. Center of plot is displaced due to vertical dispersion for both y and y'.

aperture has been reached. For these determinations the coordinates of the closed orbit must be known accurately. In PATRICIA the user selects the initial emittance ε_o of the betatron motion. The program finds the coordinates Z_{co} and Z'_{co} (Z = x or y) of the closed orbit and generates the launching conditions of the test particle:

$$Z = \sqrt{\beta_z \varepsilon_o} + Z_{co}$$

$$Z' = Z'_\beta + Z'_{co} \qquad \text{(normally } Z'_\beta = 0\text{)}.$$

Any uncertainty in the closed orbit becomes an additional betatron amplitude relative to the real closed orbit; the emittance of the particle is changed. In addition, the emittance calculated relative to an incorrect closed orbit varies as the particle progresses around the phase ellipse; there is an emittance modulation with a period of a few turns. Runs using small betatron amplitudes for $\Delta P/P \neq 0$ sometimes produce phase plots that are inconsistent with the initial betatron amplitude. A series of runs for which test particles had smaller and smaller initial amplitudes showed the phase plots did not shrink to zero size but rather

References

1. L. Schachinger, private communication
2. L. Schachinger, these proceedings.
3. A.J. Dragt, Snowmass '84 proceedings, 369.
4. E. Forest, private communication.
5. A.J. Dragt, Snowmass '86 talk.
6. S. Peggs and R. Talman, SSC-84 (1986).
7. L.R. Evans and J. Gareyte, IEEE Trans. Nucl. Sci. NS-30 (1983) 2397.
8. ibido, NS-32 (1985) 2234.
9. L. Schachinger and R. Talman, SSC-52 (1985).
10. D.C. Carey and F.C. Iselin, Proc. 1984 Summer Study on the Design and Utilization of the Superconducting Super Collider 389 (1984).
11. A.A. Garren, A.S. Kenney, E.D. Courant, M.J. Syphers, Fermilab Report FN 420 (1985).
12. B. Autin and Y. Marti, CERN ISR-MA/73-17 (1973).
13. A.J. Dragt, R.D. Ryne, L.M. Healy, F. Neri, MARYLIE 3.0. Draft Report (1985).

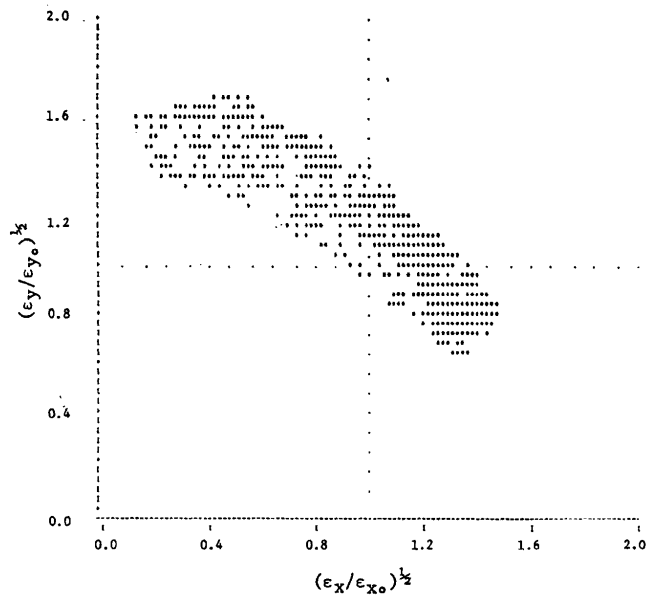

Fig. 5 Plot of $(\varepsilon_y/\varepsilon_{y_o})^{1/2}$ vs $(\varepsilon_x/\varepsilon_{x_o})^{1/2}$ on a turn by turn basis(smear plot). $\Delta P/P=0.1\%$. Coupling results in arc-like nature of plot. $(\varepsilon_x+\varepsilon_y)^{1/2} \approx$ constant. SMEAR = 0.298, SMEAR1 = .053.

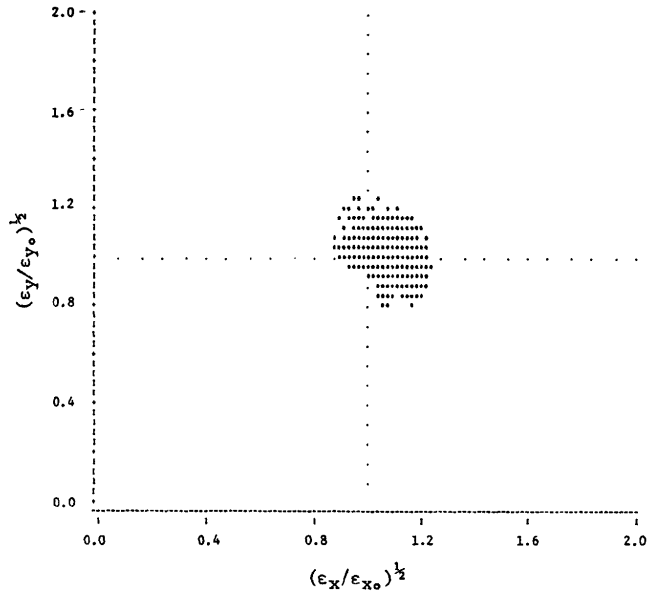

Fig. 6 Plot of $(\varepsilon_y/\varepsilon_{y_o})^{1/2}$ vs $(\varepsilon_x/\varepsilon_{x_o})^{1/2}$ on a turn by turn basis(smear plot). $\Delta P/P=-0.1\%$. Points of plot are nicely clustered and indicate little coupling. SMEAR = 0.074, SMEAR1 = 0.042.

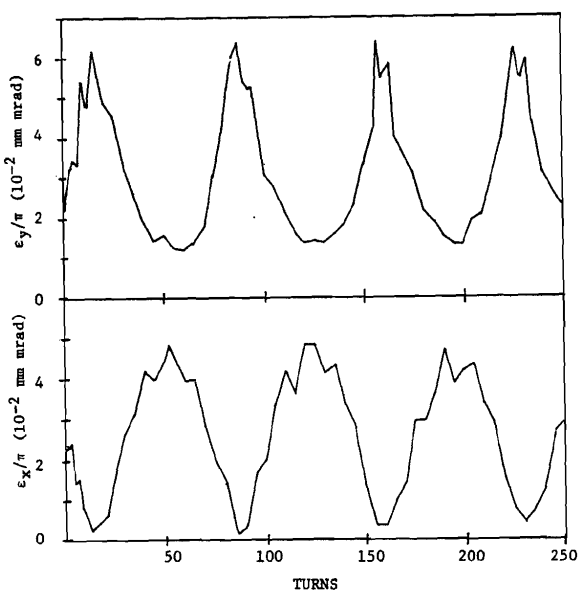

Fig. 7 Plot of the dependence of ε_x and ε_y on time (number of turns) for $\Delta P/P=0.1\%$. $\varepsilon_{x_o}=\varepsilon_{y_o} = 0.0225\pi$ mm mrad. ε_y increases rapidly from ε_{y_o} to 0.06π mm mrad. $\hat{\varepsilon}_y > \varepsilon_{x_o}+\varepsilon_{y_o}$, but $\varepsilon_t = \varepsilon_x+ \varepsilon_y \approx$ constant for times greater than 15 turns.

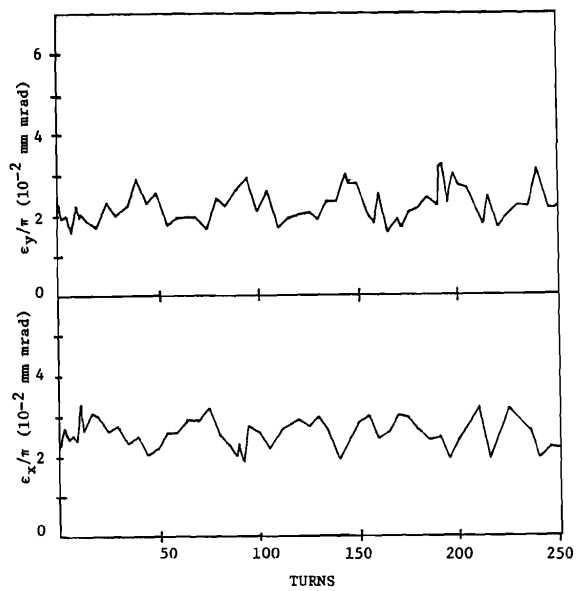

Fig. 8 Plot of the dependence of ε_x and ε_y on time (number of turns) for $\Delta P/P=-0.1\%$. $\varepsilon_{x_o}=\varepsilon_{y_o} = 0.0225\pi$ mm mrad. The sum, $(\varepsilon_x +\varepsilon_y)$, is only slightly greater than the sum of the initial emittances.

reached a minimum and then started to increase even though the initial betatron amplitude was still being decreased! The closed orbit generated by PATRICIA includes linearized contributions from higher order field components; apparently this approximation is not sufficiently accurate for the present studies. This problem has been greatly reduced by changing the program so it first tracks a very small amplitude particle for 100 turns, averages x, x', y, and y', and uses the results as the coordinates of the closed orbit.

The linear aperture can be defined on the basis of a tune shift from a particle having zero amplitude or on the basis of the smear of the dependence of $\sqrt{\varepsilon_y}$ on $\sqrt{\varepsilon_x}$ (Figs. 5 & 6). The steps used to generate a measure of the smear (called SMEAR) are listed below:[4]

1). Determine the parameters of the betatron motion ΔZ, $\Delta Z'$ relative to the closed orbit Z_{co} and and Z'_{co} for each turn. $\Delta Z_i = Z_i-Z_{co}$, $\Delta Z_i' = Z_i'-Z_{co}'$ for Z = x and y.

2). Determine the Courant-Snyder function for each turn: $\varepsilon_i = (\Delta Z_i^2 + (\alpha_z\Delta Z_i + \beta_z\Delta Z_i')^2) / \beta_z$.

3). Define $P_{zi} = \sqrt{\varepsilon_i}$, compute $\overline{P}_z$, and determine $\Delta P_{zi} = P_{zi} - \overline{P}_z$ for each turn.

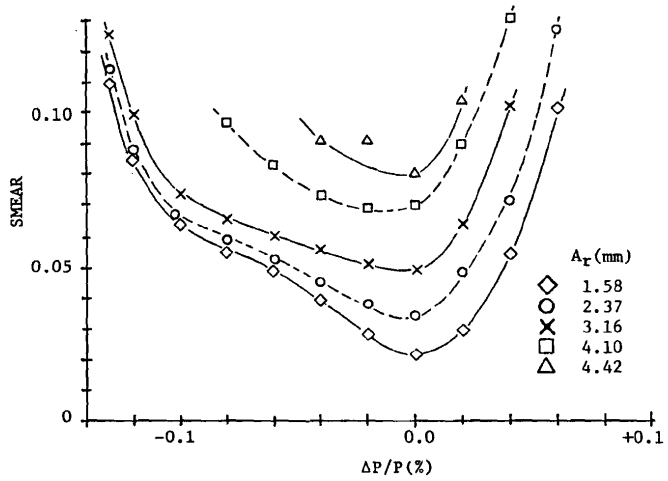

Fig. 9 Dependence of the SMEAR function on ΔP/P for several initial amplitudes. Random multipoles present in dipoles and quadrupoles in the insertions as well as in the arcs. Multipoles in the triplet Q1 to Q3 are assumed to be 90% corrected. $A_r = (x^2+y^2)^{1/2}$.

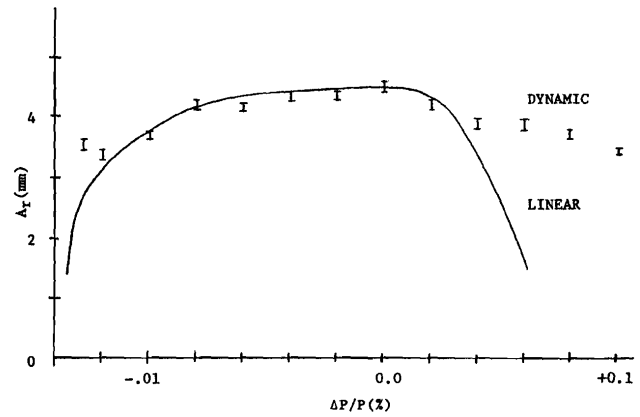

Fig. 10 Dependence of linear aperture (solid curve) on ΔP/P constructed from the data of Fig. 9. Points with bars represent the dynamic aperture. The motion is stable at the lower limit of the bars and is unstable within 1000 turns at the upper limit of the bars.

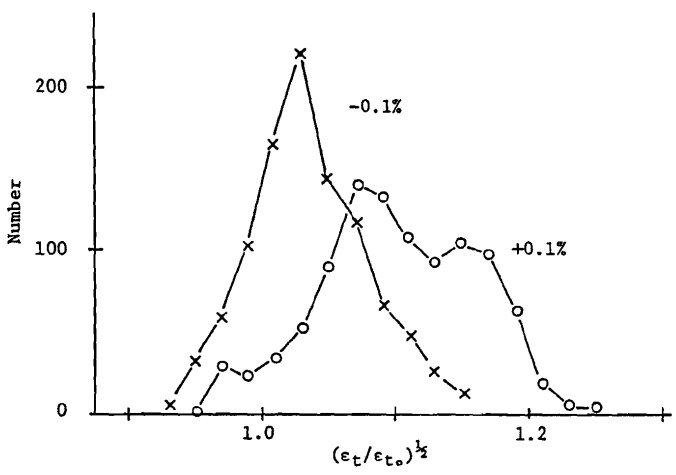

Fig. 11 Distribution of the radial dependence of $(\varepsilon_t/\ \varepsilon_{t_o})^{1/2}$ on ΔP/P for the smear plots of figures 5&6. Points are plotted at the center of histogram bins. The distribution for ΔP/P=-0.1% is sharp and has an average value of 1.04. The distribution for ΔP/P=0.1% is more complicated and indicates emittances significantly larger than the total initial emittance of $2\varepsilon_o$.

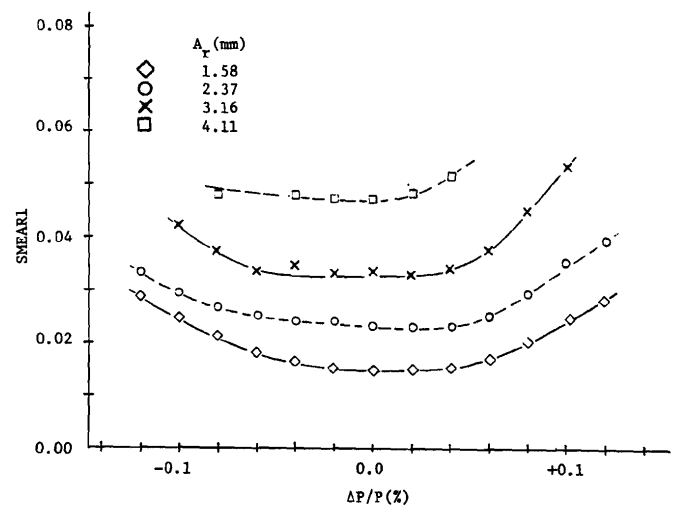

Fig. 12 Dependence of the SMEAR1 function on ΔP/P. These distributions are companions to those of Fig. 9; they were generated from the same tracking data.

4). Determine the rms deviation of the ΔP_{zi}'s.

$$\sigma P_z = (\sum \sigma P_{zi}^2/\text{TURNS})^{1/2}$$

5). Determine the SMEAR defined as:

$$\text{SMEAR} = ((\ \sigma P_x^2 + \sigma P_y^2)/(\overline{P}_x^2 + \overline{P}_y^2))^{1/2}$$

The linear aperture has been defined as that initial amplitude that gives a SMEAR of 0.1.

Five particles having different amplitudes were tracked for 1000 turns at several momenta in the range $-0.12 \leq \Delta P/P \leq 0.12\%$, and the SMEAR as defined above was evaluated and is plotted in Figure 9. From this plot the range of ΔP/P for which the SMEAR at each amplitude is less than 0.1 is determined, and the corresponding linear aperture is constructed. The results of this determination are shown in Figure 10. Also appearing on the plot is the dynamic aperture above which the motion is unstable. Several features are of interest:

1). The dynamic and linear apertures are essentially equal in the range $-0.10 \leq \Delta P/P \leq 0.03\%$,

2). The dynamic aperture is nearly symmetric around ΔP/P = 0.0% and decreases gradually as ΔP/P increases to ± 0.1%,

3). The SMEAR plots are not symmetric around ΔP/P = 0.0%,

4). The linear aperture falls off abruptly below ΔP/P = -0.12% and above 0.03%, and

5). The radial linear aperture $A_r=(x^2+y^2)^{1/2}$ measured at the center of arc quadrupoles is A_r = 4.4 mm. This is to be compared with the value of 5.5 ± 1.3 mm from the CDR[5] -- when there were magnet errors in the arc dipoles only. In that case the dynamic aperture quoted is 9.1 ± 1.5 mm, while for the present study in which multipoles are included in the insertion dipoles and quadrupoles, the linear and dynamic apertures are equal.

For purposes of comparison, runs have also been made when there are random multipoles in the arc dipoles only. The dependence of the SMEAR function on momentum is shown in Figure 13, and the radial linear and dynamic apertures are plotted on Figure 14 (radial aperture $A_r = (x^2 + y^2)^{1/2} = (\varepsilon(\beta_x + \beta_y))^{1/2}$). At $\Delta P/P=0$, the linear aperture is 7.8 mm and the dynamic aperture is 9.9 mm. The linear aperture is larger while the dynamic aperture agrees with the values quoted in the CDR.

Alternate Criterion for the Linear Aperture

The linear aperture obtained from the SMEAR function is essentially equal to the dynamic aperture for $-0.10 \leq \Delta P/P \leq 0.03\%$. This seems surprising. Also surprising are the large values of SMEAR for $\Delta P/P > 0\%$.

Reconsidering the smear plots of Figures 5 & 6, it is noted that the radial distance of any point from the origin is $(\varepsilon_x + \varepsilon_y)^{1/2} = (\varepsilon_t)^{1/2}$, the square root of the total emittance. The elongated distribution of Figure 5 suggests an arc of a circle upon which ε_t is constant. This corresponds to motion with the total emittance invariant as emittance is transferred back and forth between the two planes. The transfer causes periodic increases in the beam size in each plane, but this transfer is limited in magnitude. Perhaps a more realistic measure of the nonlinearity of the smear distribution is its rms radial variation. In Figure 11 the distribution of $(\varepsilon_t/\varepsilon_{to})^{1/2}$ is plotted for the smear distributions of Figures 5 & 6. The curves are generated from histograms with the points located at the center of each bin. The distribution for $\Delta P/P = -.1\%$ approximates a gaussian, while that for $\Delta P/P = +.1\%$ has a more complicated structure that reflects the large emittance in the vertical plane (Fig. 7). Following steps similar to those leading to the SMEAR function, an alternate function, SMEAR1, derived from the rms variation of $\varepsilon_t^{1/2}$ is suggested:

$$\text{SMEAR1} = \sigma(\varepsilon_t^{1/2}) / \overline{\varepsilon_t^{1/2}}$$

The dependence of SMEAR1 on momentum is shown in Figure 12 for the same data used to generate Figure 9. In this case the SMEAR1 function never reaches the limit of 0.1; that is, the dynamic aperture limits the motion.

Linear Aperture Determined from Tune Shift

The linear aperture based on the tune shift from a small amplitude oscillation has been determined when there are random multipoles in the dipoles and quadrupoles of both the arcs and the insertions. The tune of the betatron motion at any initial amplitude is determined by averaging the rotation of the particle around the normalized phase ellipse. Tunes were considered valid only when the tracking run went to completion (1000 turns). The tune dependence on amplitude was determined at each momentum, and the amplitude where $\Delta\nu = 0.005$ was obtained by interpolation. The resulting dependence of aperture on $\Delta P/P$ is shown in Figure 15. At $\Delta P/P = 0$, the linear aperture is ≃ 4.1 mm, and it is 3.8 mm and 2.61 mm at $\Delta P/P = +0.1$ and -0.1%, respectively. Thus the linear aperture based on tune shift does not show the same momentum dependence as that obtained from the SMEAR criterion (Fig. 10).

The determination of linear aperture based on the tune shift was also made when the head-on beam-beam effect was included. At each crossing point the test particle was given a kick appropriate to the β^* and its radial position. The tune at small amplitudes was decreased and is shown in Figure 16. The tracking results at large amplitudes were unchanged. It seems appropriate to use the small amplitude tune without the head-on beam-beam effect as the reference tune. When this is done, the linear aperture derived from the tune shift is unchanged from that of Figure 15.

Conclusion

In the present study the criteria of SMEAR, SMEAR1 and $\Delta\nu \leq 0.005$ are used to determine the momentum dependence of the linear aperture of the SSC storage lattice, and the results are compared with the linear and dynamic apertures listed in the CDR. There is a difference in the results that arises from different techniques being used by different people[5,6,7]. All apertures of the present paper are radial apertures A_r with $A_r = (\varepsilon(\beta_x+\beta_y))^{1/2}$ and β_x and β_y measured at the same quadrupole; they are consistent with the radial apertures of Reference 7.

The apertures of References 5&6 were obtained from runs on test lattices (no vertically deflecting beam crossing dipoles) and were determined as $A = (\varepsilon(\hat{\beta}_x+\hat{\beta}_y)^{1/2}$ where $\hat{\beta}_x$ and $\hat{\beta}_y$ are maximum values measured at horizontally and vertically focusing quadrupoles, respectively. Thus these apertures are thought to be high by 22% ($\beta_x(QF)=\beta_y(QD)=330$m and $\beta_y(QF)=\beta_x(QD)=110$m).

The criterion used in Reference 5 to estimate the linear aperture from the smear distribution is different from that used in the present study. Defining $A_z=\varepsilon_z^{1/2}$ for z=x and y, and with ΔA_z being the range of A_z, and with ΔA being the larger of ΔA_x and ΔA_y, their criterion for the linear aperture is:

$$2\Delta A/(\overline{A}_x^2 + \overline{A}_y^2)^{1/2} = 0.3$$

This criterion should be satisfied at smaller amplitudes than those satisfying the SMEAR = 0.1 criterion. This smaller amplitude is at least partially compensated by the 22% overestimate in converting amplitudes to aperture. With differences in lattices and techniques, the only real comparison that can be made is the dynamic aperture of References 5&6 with that of the current study when multipoles are present in the arc dipoles only. Their values of 9.1±1.5 and 10.1± 1.3 mm agree well with the value of 9.9 mm of the present work. Reduction of their values by 22% would destroy this agreement.

The SMEAR1 function is a measure of the rms variation of $\varepsilon_t^{1/2}$ and is less sensitive to coupling than is the SMEAR function. For the present studies SMEAR1 ≤.1 gives a linear aperture nearly equal to the dynamic aperture. It is possible that the SMEAR1 function is the appropriate way to evaluate the linear aperture but that the allowed limit should be reduced to 0.03 or less. The relative merits of SMEAR, SMEAR1 and the tune shift criterion warrant further study.

Finally, a comment is made about the concept of a dynamic aperture. This aperture is defined by the largest amplitude betatron motion that survives for a specified number of turns-- no radial constraint is imposed on the motion. This aperture has been used as a tool to compare the performance of different lattices.

The triplet quadrupoles have large beta functions ($10{,}000 \leq (\beta_x+\beta_y) \leq 13{,}000$ for $-0.12 \leq \Delta P/P \leq +0.12\%$ A radial amplitude of 5 mm in an arc quadrupole corresponds to an amplitude of 25 to 30 mm in the triplets.

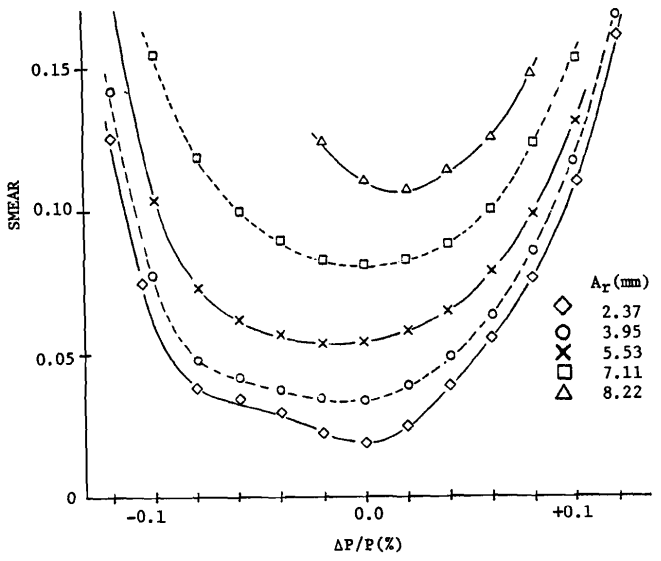

Fig. 13 SMEAR distribution for a study having random multipoles in the arc dipoles only. This study was made to permit direct comparison of the present work with the data presented in the CDR.

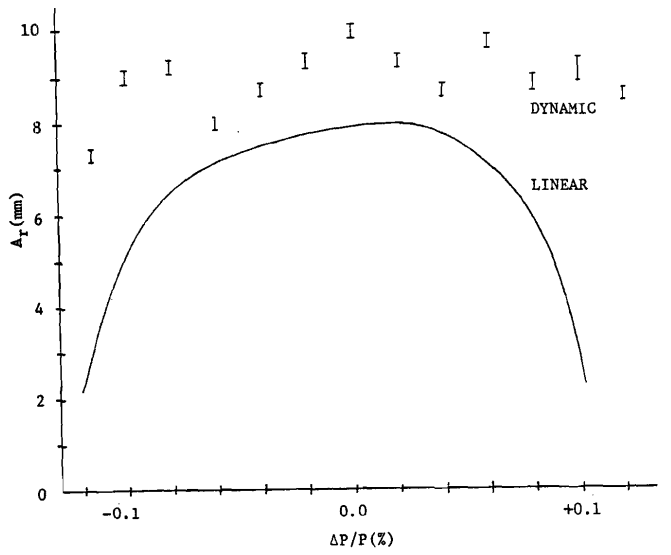

Fig. 14 Linear aperture (solid) constructed from the SMEAR distributions of Fig. 13. Also shown is the dynamic aperture (bars) for the same study. The linear aperture is 7.8 mm and the dynamic aperture is 9.9 mm at ΔP/P=0% as compared with the values of 5.5± 1.3 mm and 9.1 ± 1.5 mm reported in the CDR.

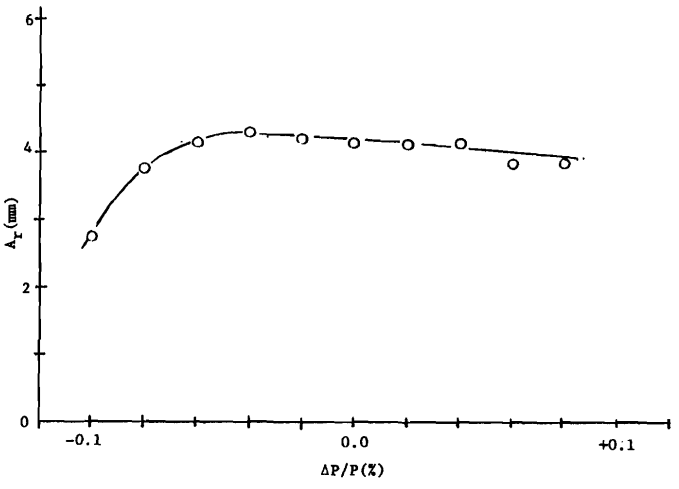

Fig. 15 Linear aperture usion the criterion that $\nu(\Delta P/P)-\nu(0,0) \leq 0.005$ where $\nu(0,0)$ denotes the betatron tune derived from a small amplitude oscilattion at ΔP/P=0.0%.

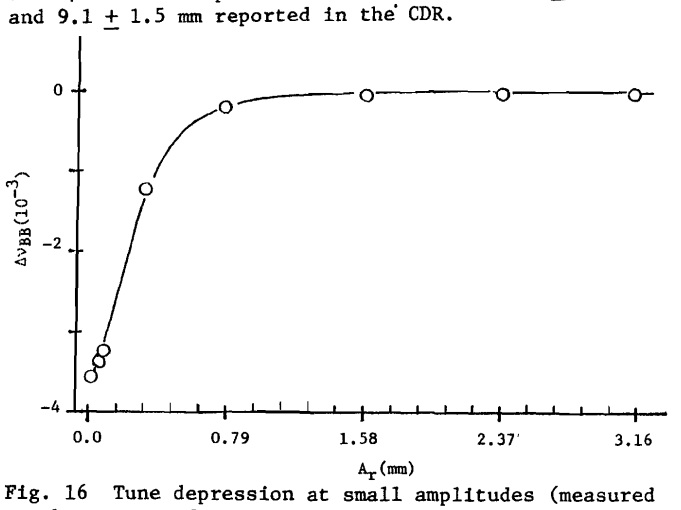

Fig. 16 Tune depression at small amplitudes (measured at the center of a horizontally focusing arc quadrupole) when the head-on beam-beam effect is included.

When the 100% coupling of Figure 1 is included, the beam size in the triplets is increased by an additional factor of $\sqrt{2}$. The coil ID of the triplets is 4 cm. Even without coupling, a 5 mm amplitude in the arcs is magnified to an amplitude in the triplets that exceeds their inner coil radius; the situation is even worse when coupling is present. The random multipole coefficients scale with order n as $1/r_o^{n+m}$ with r_o being an average coil radius and $m=\frac{1}{2}$ for dipoles and $m=-\frac{1}{2}$ for quadrupoles. For amplitudes greater than r_o, the multipole expansion of the field is no longer valid--the importance of multipoles increases with increasing order, while in the region where the field expansion is valid, the opposite is the case. The region where $r>r_o$ is unphysical; large kicks are given to the test particle so that the motion, when it diverges, does so in a fraction of a turn. When random multipoles are present in the arc dipoles only, the dynamic aperture is consistent with the test particle staying within the beam pipe throughout the arcs. The test particle does make large excursions in the insertions, but there it experiences no kicks due to multipoles. In this case the dynamic aperture is less than the acceptance of the arcs, and it has physical significance. When multipoles are included in the insertions, one is using a region where the field expansion is not valid, and the dynamic aperture loses its significance. In this case the acceptance (physical aperture) is the meaningful quantity.

References

1). G.F. Dell, IEEE Transactions on Nuclear Science, Vol. NS-32, No. 5, 1985, pp. 1623-1625.

2). SSC Conceptual Design Report, SSC-SR-2020, Mar. 1986

3). ibid. pp. 127 and 128.

4). D. Edwards, FNAL, Private Communication.

5). Conceptual Design Report, op. cit. pg. 136.

6). ibid. pg. 139.

7). ibid. pp. 157-159.